Journal of Oral Biosciences 65 (2023) 97–103

Contents lists available at ScienceDirect

Journal of Oral Biosciences

journal homepage: www.elsevier.com/locate/job

Original Article

# Hydrogen peroxide-induced oxidative stress promotes expression of CXCL15/Lungkine mRNA in a MEK/ERK-dependent manner in fibroblast-like synoviocytes derived from mouse temporomandibular joint

Kanna Asanuma [a, b], Seiji Yokota [a], Naoyuki Chosa [a], Masaharu Kamo [a], Miho Ibi [c], Hisayo Mayama [b], Tarou Irié [c], Kazuro Satoh [b], Akira Ishisaki [a, *]

[a] Division of Cellular Biosignal Sciences, Department of Biochemistry, Iwate Medical University, 1-1-1 Idai-dori, Yahaba-cho, Shiwa-gun, Iwate-ken 028-3694, Japan
[b] Division of Orthodontics, Department of Developmental Oral Health Science, Iwate Medical University, 1-3-27 Chuo-dori, Morioka-shi, Iwate-ken 020-8505, Japan
[c] Division of Anatomical and Cellular Pathology, Department of Pathology, Iwate Medical University, 1-1-1 Idai-dori, Yahaba-cho, Shiwa-gun, Iwate-ken 028-3694, Japan

ARTICLE INFO

*Article history:*
Received 24 October 2022
Accepted 19 December 2022
Available online 28 December 2022

*Keywords:*
Oxidative stress
CXCL15
MEK/ERK
Fibroblast-like synoviocytes
Temporomandibular joint

ABSTRACT

*Objectives:* Temporomandibular joint osteoarthritis (TMJ-OA) is a multifactorial disease caused by inflammation and oxidative stress. It has been hypothesized that mechanical stress-induced injury of TMJ tissues induces the generation of reactive oxygen species (ROS), such as hydroxyl radical (OH•), in the synovial fluid (SF). In general, the overproduction of ROS contributes to synovial inflammation and dysfunction of the subchondral bone in OA. However, the mechanism by which ROS-injured synoviocytes recruit inflammatory cells to TMJ-OA lesions remains unclear.
*Methods:* Reverse transcription-quantitative polymerase chain reaction (RT-qPCR) was performed to evaluate the mRNA expression of chemoattractant molecules. The phosphorylation levels of intracellular signaling molecules were evaluated using western blot analysis.
*Results:* Hydrogen peroxide ($H_2O_2$) treatment significantly promoted mRNA expression of neutrophil chemoattractant CXCL15/Lungkine in a dose-dependent manner (100–500 μM) in fibroblast-like synoviocytes (FLSs) derived from mouse TMJ. $H_2O_2$ (500 μM) significantly upregulated the phosphorylation of extracellular signal-regulated kinase (ERK)1 and ERK2 in FLSs. Intriguingly, the mitogen-activated protein (MAP)/ERK kinase (MEK) inhibitor U0126 (10 μM) nullified $H_2O_2$-induced increase in CXCL15/Lungkine mRNA expression. Additionally, $H_2O_2$ (500 μM) administration significantly upregulated OH• production in FLSs, as assessed by live-cell permeant fluorescent probe targeted against OH• under fluorescence microscopy. Furthermore, the ROS inhibitor *N*-acetyl-L-cysteine (5 mM) partially but significantly reversed $H_2O_2$-mediated phosphorylation of ERK1/2.
*Conclusions:* $H_2O_2$-induced oxidative stress promoted the expression of CXCL15/Lungkine mRNA in a MEK/ERK-dependent manner in mouse TMJ-derived FLSs, suggesting that FLSs recruit neutrophils to TMJ-OA lesions through the production of CXCL15/Lungkine and exacerbate the local inflammatory response.


*Abbreviations:* OA, osteoarthritis; TMJ, temporomandibular joint; ROS, reactive oxygen species; IL, interleukin; GSH, glutathione; CCL, chemokine (C–C motif) ligand; OH•, hydroxyl radical; $H_2O_2$, hydrogen peroxide; MAPK, mitogen-activated protein kinase; ERK, extracellular signal-regulated kinase; JNK, c-jun $NH_2$-terminal kinase; PI3K, phosphoinositide 3-kinase; CXCL, chemokine (C-X-C motif) ligand; MEK, MAP/ERK kinase; SV40LT, simian virus 40 large T antigen; GAPDH, glyceraldehyde-3-phosphate dehydrogenase; NAC, *N*-acetyl-L-cysteine.

* Corresponding author. Division of Cellular Biosignal Sciences, Department of Biochemistry, Iwate Medical University, 1-1-1 Idai-dori, Yahaba-cho, Shiwa-gun, Iwate-ken 028-3694, Japan. Tel.: +81-19-651-5111; Fax: +81-19-908-8012.
*E-mail address:* aishisa@iwate-med.ac.jp (A. Ishisaki).

https://doi.org/10.1016/j.job.2022.12.002

## 1. Introduction

Osteoarthritis (OA) of the temporomandibular joint (TMJ) is a degenerative disease that is accompanied by dysfunction and severe pain [1]. The pathogenesis of OA is affected by environmental factors that are correlated with the activation of molecular mechanisms that promote progression of articular injury [2]. TMJ-OA is a multifactorial disease that is induced by inflammation [3,4]. Progression of OA is associated with reactive oxygen species (ROS) and oxidative stress [5,6]. Intriguingly, interleukin-1 beta (IL-1β), a pro-inflammatory cytokine, induces the expression of inflammatory mediators, such as IL-6, inducible nitric synthase, and cyclooxygenase-2, and enhances ROS levels in human TMJ chondrocytes [7], suggesting that IL-1β strengthens the inflammatory response and exacerbates oxidative stress in TMJ-OA lesions. ROS signaling pathway is a new therapeutic target for OA treatment. Consistently, Setti et al. reported that the major antioxidant glutathione (GSH) and its precursor *N*-acetylcysteine exerted significant protective effects against tissue injury by exacerbating oxidative stress in chronic inflammatory diseases, such as OA [8].

In general, the production of chemokines contributes to inflammatory progression in OA lesions; chemokines produced in OA lesions promote chemotactic activity in inflammatory cells, such as neutrophils, macrophages, and lymphocytes, and facilitate the recruitment of these inflammatory cells into OA lesions, resulting in further production of pro-inflammatory cytokines from the recruited inflammatory cells [9]. Molnar et al. reported that IL-1β promotes the expression of chemokines, including neutrophil chemoattractant IL-8, monocyte chemoattractant protein-1/chemokine (C–C motif) ligand 2 (CCL2), and T-cell-, macrophage-, eosinophil-, and basophil-chemoattractant CCL5/RANTES in OA lesions [9]. Intriguingly, hydroxyl radicals (OH•) and hydrogen peroxide ($H_2O_2$) also induce expression of IL-8 and intercellular adhesion molecule-1 in endothelial cells, and subsequently promote extravasation of neutrophils [10]. In addition, $H_2O_2$ treatment significantly induces IL-8 expression through the activation of mitogen-activated protein kinases (MAPKs), including extracellular signal-regulated kinase (ERK), p38 MAPK, and c-Jun $NH_2$-terminal kinase (JNK) in human periodontal ligament cells [11]. In contrast, Luigi et al. demonstrated that $H_2O_2$ stimulation significantly induced IL-8 expression in fibroblasts derived from systemic sclerosis patients in a phosphoinositide 3-kinase (PI3K)/Akt-dependent manner [12]. Consistently, Jeong et al. reported that $H_2O_2$ treatment significantly increased IL-8 expression in a PI3K/Akt-dependent manner [13]. However, whether oxidative stress promotes the expression of neutrophil chemoattractants, such as IL-8, in TMJ-OA lesions in a MAPKs- or PI3K/Akt-dependent manner remains to be clarified.

The chemokine (C-X-C motif) ligand (CXCL) family plays an important role in the progression of inflammation [14]. CXCL15/Lungkine, which is mapped to mouse chromosome 5, was identified as a homolog of human IL-8 and promotes chemotactic activity in neutrophils both *in vitro* and *in vivo*. Intraperitoneal injection of CXCL15/Lungkine increases the number of neutrophil marker Gr-1-positive cells in the peritoneum. In addition, a transwell chemotaxis assay revealed that CXCL15/Lungkine induced neutrophil migration in a dose-dependent manner [15]. Histopathological analysis of CXCL15/Lungkine null mice revealed that CXCL15/Lungkine is an important factor that regulates neutrophil migration from the lung parenchyma into the airspace [16]. A recent study showed that CXCL15/Lungkine, previously reported to be a lung-specific chemokine, was also highly expressed in murine gastrointestinal, urogenital, and endocrine organs [17]. However, whether CXCL15/Lungkine plays an important role in the progression of TMJ-OA remains to be clarified.

Here, we evaluated whether the IL-8 inducer $H_2O_2$ promotes CXCL15/Lungkine mRNA expression in the mouse TMJ-derived FLS cell line FLS1 [18], and whether MAPKs- or PI3K/Akt-mediated intracellular signals play an important role in the $H_2O_2$-mediated expression of CXCL15/Lungkine mRNA. Additionally, this study aimed to identify molecular targets for the establishment of novel therapies that suppress the development of inflammatory lesions in TMJ-OA.

## 2. Materials and methods

### 2.1. Cell culture

The FLS cell line FLS1 was previously established from synovial tissue collected from the mouse TMJ. FLS1 cells were immortalized by transfection with the simian virus 40 large T antigen (SV40LT) expression vector [18]. Cells were cultivated in Ham's F-12 growth medium supplemented with 10% fetal bovine serum (FBS), 2 mM L-glutamine, penicillin (100 units/mL), and streptomycin (100 μg/mL). The cells were incubated in a 5% $CO_2$ and 20% $O_2$ environment at 37 °C and subcultured at a ratio of 1:4 when the cells reached subconfluency.

### 2.2. Materials

Ham's F-12 medium was purchased from Sigma–Aldrich (St. Louis, MO, USA). L-glutamine (200 mM), penicillin-streptomycin (100 x), and alamarBlue® Cell Viability Reagent were purchased from Invitrogen (Carlsbad, CA, USA). Hydrogen peroxide was purchased from Nacalai Tesque Inc. (Kyoto, Japan). The MAP/ERK kinase (MEK) inhibitor U0126, p38 MAPK inhibitor SB203580, and PI3K inhibitor LY294002 were purchased from Merck KGaA (Darmstadt, Germany). *N*-acetyl-L-cysteine (NAC) was purchased from Sigma–Aldrich (St. Louis, MO, USA). Rabbit polyclonal antibodies p44/42MAPK (Erk1/2) (#9102S), phospho-p44/42 MAPK (Erk1/2) (Thr202/Tyr204) (#9101S), p38 MAPK (#9212S), phospho-p38 MAPK (Thr180/Tyr182) (#9211S), SAPK/JNK (#9252S), Akt (#9272S), and phospho-Akt (Ser473) (#9271S), and rabbit monoclonal antibodies phospho-SAPK/JNK (Thr183/Tyr185) (#9255S), and glyceraldehyde-3-phosphate dehydrogenase (GAPDH) (#5174S) were purchased from Cell Signaling Technology, Inc. (Danvers, MA, USA). Importantly, phosphorylation of ERK1 and ERK2 (ERK1/2) at Thr202/Tyr204, that of p38 MAPK at Thr180/Tyr182, that of JNK at Thr183/Tyr185, and that of Akt at Ser473 were required for activation of these enzymes [19–22]. The Cell Meter™ mitochondrial hydroxyl radical detection kit (red fluorescence) was purchased from AAT Bioquest, Inc. (Sunnyvale, CA, USA). Hoechst 33342 was purchased from FUJIFILM Wako PURE Chemical Corp (Osaka, JAPAN).

### 2.3. Cell viability assay

Cell viability assay was performed using the oxidation-reduction indicator alarmarBlue® (resazurin). Briefly, $1 \times 10^4$ FLS1 cells/well were seeded into 96-well plates in growth medium and incubated for 24 h. Then, the growth medium was replaced with growth medium with or without $H_2O_2$ (100–1000 μM), and the cells were incubated for 24 h. Subsequently, the growth medium was replaced with growth medium containing alarmarBlue® reagent (10% (v/v)), and the cells were incubated for 4 h. Absorbance was then measured using a plate reader (Tosoh Corp., Tokyo Japan) at $Abs_{570}$ (reduced form) and $Abs_{600}$ (oxidized form). Cell viability was calculated as the percentage of control cells that were cultured without $H_2O_2$.

### 2.4. Reverse transcription-quantitative polymerase chain reaction (RT-qPCR)

FLS1 cells ($0.8 \times 10^5$ cells/well) were seeded in 12-well plates with growth medium. After 24 h of incubation, the medium was replaced with growth medium with or without $H_2O_2$ at the indicated concentrations. The cells were further incubated for 24 h. Total RNA was extracted from FLS1 cells using ISOGEN reagent (Nippon Gene Co., Ltd., Toyama, Japan). After removing the proteins from the sample solution containing the extracted total RNA using the phenol extraction method, first-strand complementary DNA (cDNA) was synthesized from the extracted total RNA using PrimeScript™ RT reagent Master Mix (Takara Bio Inc., Shiga, Japan). Subsequently, qPCR for cDNA amplification was performed in a Thermal Cycler Dice Real Time System (Takara Bio Inc.) with SYBR Premix Ex Taq II (Takara Bio Inc.). The primers used for cDNA amplification were as follows: *CXCL15*/*Lungkine* forward, 5′-GGCAAGAACACTGTGTCCAAAGA-3′ and reverse, 5′-GTGGATGACTGTCCATGCAGAA-3′; *GAPDH* forward, 5′- TGTGTCC GTCGTGGATCTGA-3′ and reverse: 5′- TTGCTGTTGAAGTCGCAGGAG-3′. *GAPDH* expression was used as an internal control.

### 2.5. Western blot

FLS1 cells ($5 \times 10^5$ cells) were seeded in 6-cm dishes with growth medium. After 24 h of incubation, the growth medium was replaced with FBS-free starvation medium, and the cells were maintained for 24 h. The cells were then cultured with or without $H_2O_2$ (500 μM) for the indicated times. Total protein was extracted from FLS1 cells using RIPA cell lysis buffer (50 mM Tris–HCl (pH 7.2), 150 mM NaCl, 1% NP-40, 0.5% sodium deoxycholate, and 0.1% sodium dodecyl sulfate (SDS) [Nacalai Tesque Inc.]) supplemented with protease and phosphatase inhibitor cocktail (Sigma–Aldrich). Equal amounts of extracted total protein were loaded onto 12.5% SDS–PAGE gels and separated. The separated proteins were transferred onto polyvinylidene difluoride membranes (Merck KGaA). The membranes were incubated with the primary antibodies described in Section 2.2. *Materials* overnight at 4 °C according to the manufacturer's protocol. The membranes were then incubated with an alkaline phosphatase–conjugated secondary antibody for 1 h at room temperature. The targeted bands on the membrane were visualized using an alkaline phosphatase substrate kit (BCIP/NBT Substrate Kit) (SeraCare Life Science, Inc., Milford, MA, USA). The band intensity on the membrane was determined using the ImageJ 1.53a software (National Institutes of Health, Bethesda, MD, USA).

### 2.6. Hydroxyl radical detection

Detection of hydroxyl radicals in FLS1 cells was performed using a Cell Meter™ mitochondrial hydroxyl radical (OH•) detection kit under a fluorescence microscope. Briefly, FLS1 cells ($0.07 \times 10^5$ cells/well) were seeded in 96-well plates with growth medium and maintained for 24 h. The growth medium was then replaced with that containing the permeant probe MitoROS™ OH580, which targets OH•, and emits red fluorescent light. The cells were incubated for 1 h. Nuclei were also counter-stained with Hoechst 33342 (FUJIFILM Wako PURE Chemical Corp). Subsequently, the growth medium was replaced with growth medium with or without $H_2O_2$ (500 μM) and further maintained for 24 h. Finally, the change in red fluorescence intensity was monitored using an all-in-one fluorescence microscope BZ-X710 with Cy3/TRITC filter set (Keyence Co., Ltd., Osaka, Japan). For the quantitative analysis of OH• production levels in FLS1 cells, fluorescence RGB color images were taken and quantitatively evaluated using an all-in-one fluorescence microscope BZ-X analyzer.

### 2.7. Statistical analysis

All experiments were repeated at least two times, and we confirmed that we got same results. Data are presented as the mean ± standard deviation and were analyzed using SPSS software (IBM, Armonk, NY, USA). Tukey's multiple comparison test was performed to determine statistical significance, except for the data analysis shown in Fig. 4Ac. In Fig. 4Ac, the data were analyzed using Student's *t*-test. Statistical significance was set at $P < 0.05$.

## 3. Results

### 3.1. $H_2O_2$ upregulates mRNA expression of CXCL15/Lungkine in FLS1 cells in a dose-dependent manner

We examined the effect of $H_2O_2$ (100–1000 μM) on FLS1 cell viability. alarmarBlue® analysis revealed that 24 h treatment with 500 μM, 700 μM, and 1000 μM of $H_2O_2$ significantly decreased the viability of FLS1 cells in a dose-dependent manner (500 μM, 90%; 700 μM, 48.4%; and 1000 μM, 0%); however, 100–300 μM $H_2O_2$ did not affect cell viability (Fig. 1A). Therefore, we decided to 100–500 μM $H_2O_2$ for subsequent experiments.

We found that $H_2O_2$ (100–500 μM) promoted mRNA expression of CXCL15/Lungkine in FLS1 cells in a dose-dependent manner (Fig. 1B).

### 3.2. $H_2O_2$ treatment increases phosphorylation of ERK1/2, p38 MAPK, and Akt in FLS1 cells

We found that $H_2O_2$ (500 μM) promoted the phosphorylation of ERK1/2 in FLS1 cells; upregulation of ERK1/2 phosphorylation started at 10 min after $H_2O_2$ treatment, increased thereafter, and peaked at 30 min after $H_2O_2$ treatment (Fig. 2A). We also found that $H_2O_2$ (500 μM) significantly promoted phosphorylation of p38 MAPK in FLS1 cells; upregulation of p38 MAPK phosphorylation started at 10 min after treatment, increased thereafter, and peaked at 30 min after $H_2O_2$ treatment (Fig. 2B). In addition, we found that $H_2O_2$ (500 μM) promoted phosphorylation of Akt in FLS1 cells 10–30 min after treatment, and that the phosphorylation level decreased 60–120 min after treatment (Fig. 2C). In contrast, JNK phosphorylation was not detectable by western blot analysis (data not shown).

### 3.3. MEK inhibitor and neither p38 MAPK inhibitor nor PI3K inhibitor suppresses $H_2O_2$-mediated mRNA expression of CXCL15/Lungkine in FLS1 cells

We confirmed that $H_2O_2$ (500 μM)-mediated increase in ERK1/2 phosphorylation was abrogated by pretreatment with the MEK inhibitor U0126 (10 μM) (Fig. 3A). We also confirmed that $H_2O_2$ (500 μM)-mediated increase in Akt phosphorylation was abrogated by pretreatment with the PI3K inhibitor LY294002 (10 μM) (Fig. 3B). We found that $H_2O_2$ (500 μM)-mediated increase in CXCL15/Lungkine mRNA expression was clearly suppressed by pretreatment with the MEK inhibitor U0126 (10 μM) (Fig. 3C). Unexpectedly, neither p38 MAPK inhibitor SB203580 (10 μM) nor PI3K inhibitor LY294002 (10 μM) suppressed $H_2O_2$-mediated increase in CXCL15/Lungkine mRNA expression (Fig. 3D and E, respectively).

### 3.4. Antioxidant NAC partially and significantly reverses the $H_2O_2$-mediated increase in phosphorylation of ERK1/2 in FLS1 cells

The HO• detection assay revealed that $H_2O_2$ (500 μM) significantly increased HO• production in FLS1 cells (Fig. 4Aa, Ab, and Ac).

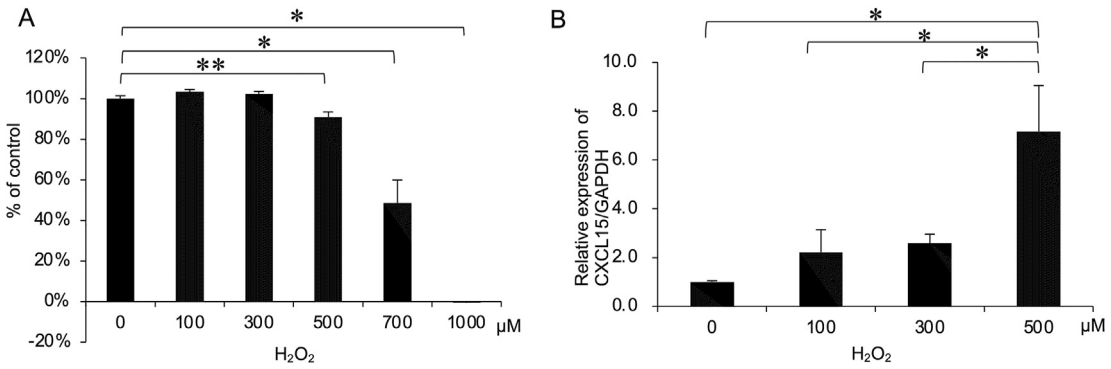


**Fig. 1.** $H_2O_2$ treatment induced mRNA expression of CXCL15/Lungkine in FLS1 cells in a dose-dependent manner. (A) Cell viability assay was performed as described in the Materials and methods section. The absorbance in each well at $Abs_{570}$ (reduced form) and $Abs_{600}$ (oxidized form) was measured using a plate reader. Cell viability was calculated as % of control cells that were not treated with $H_2O_2$. Data are presented as the mean ± standard deviation (SD) (n = 8). *, $P < 0.01$; **, $P < 0.05$. **(B)** Expression of CXCL15/Lungkine mRNA was evaluated by RT-qPCR analysis as described in the Materials and methods section. Cells were treated with $H_2O_2$ at the indicated concentrations. Data are presented as the mean ± standard deviation (SD) (n = 4). *, $P < 0.01$.

In addition, the antioxidant NAC (3–5 mM) partially and significantly suppressed $H_2O_2$ (500 μM)-mediated increase in ERK/1/2 phosphorylation in FLS1 cells; however, a lower concentration of NAC (1 mM) did not exert the same effect (Fig. 4B).

## 4. Discussion

We found that $H_2O_2$ treatment at high concentrations (≥500 μM) suppresses cell viability to 10–100% of that of control cells (Fig. 1A), suggesting that $H_2O_2$ administration at high concentrations (≥500 μM) induces oxidative stress in FLS1 cells. Consistently, we found that $H_2O_2$ (500 μM) promoted HO• production in FLS1 cells (Fig. 4Aa, Ab, and Ac). Ueno et al. demonstrated that $H_2O_2$ (100 μM) reduces the viability of TMJ-derived chondrocytes, and this was significantly abrogated by NAC treatment (2.5–5 mM) [23], suggesting that $H_2O_2$ induces oxidative stress in TMJ chondrocytes. Hiran et al. previously demonstrated that superoxide anions, which are thought to be the dominant ROS

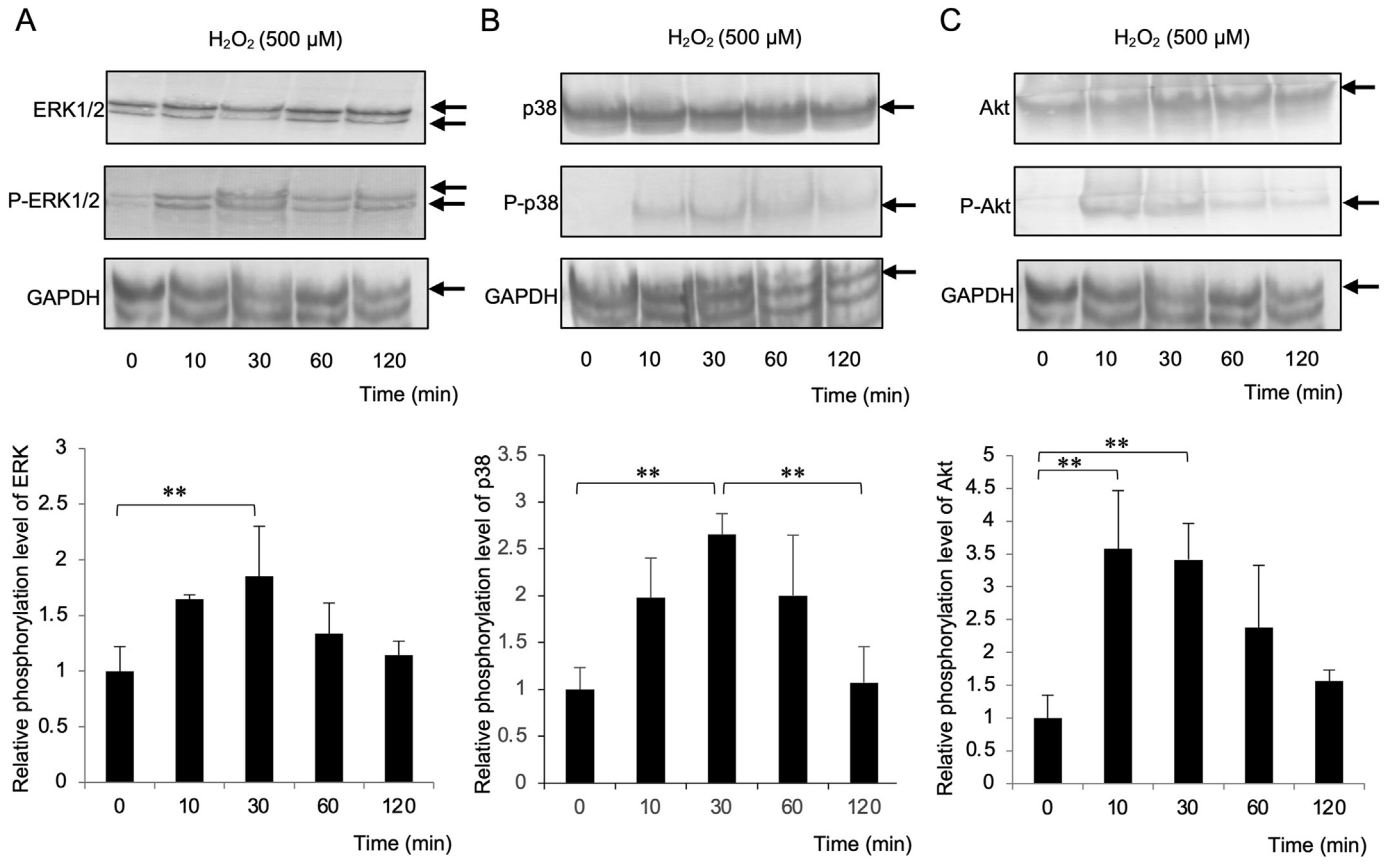


**Fig. 2.** $H_2O_2$ treatment increased phosphorylation of ERK1/2, p38 MAPK, and Akt in FLS1 cells. Western blot analysis was performed as described in the Materials and methods section. Cells were treated with $H_2O_2$ (500 μM) for the indicated time. **(A)** Total (upper panel) and phosphorylated (middle panel) ERK1/2 levels were evaluated. Relative levels of phosphorylated ERK1/2 against total levels of ERK1/2 were shown as the ratio of band intensity. **(B)** Total (upper panel) and phosphorylated (middle panel) p38 MAPK levels were evaluated. Relative levels of phosphorylated p38 MAPK against total levels of p38 MAPK were shown as the ratio of band intensity. **(C)** Total (upper panel) and phosphorylated (middle panel) Akt levels were evaluated. Relative levels of phosphorylated Akt against total levels of Akt were shown as the ratio of band intensity. **(A, B, and C)** Data are presented as the mean ± SD (n = 3). **, $P < 0.05$. GAPDH levels (lower panel) were examined as a reference for the amount of protein loaded in each lane.

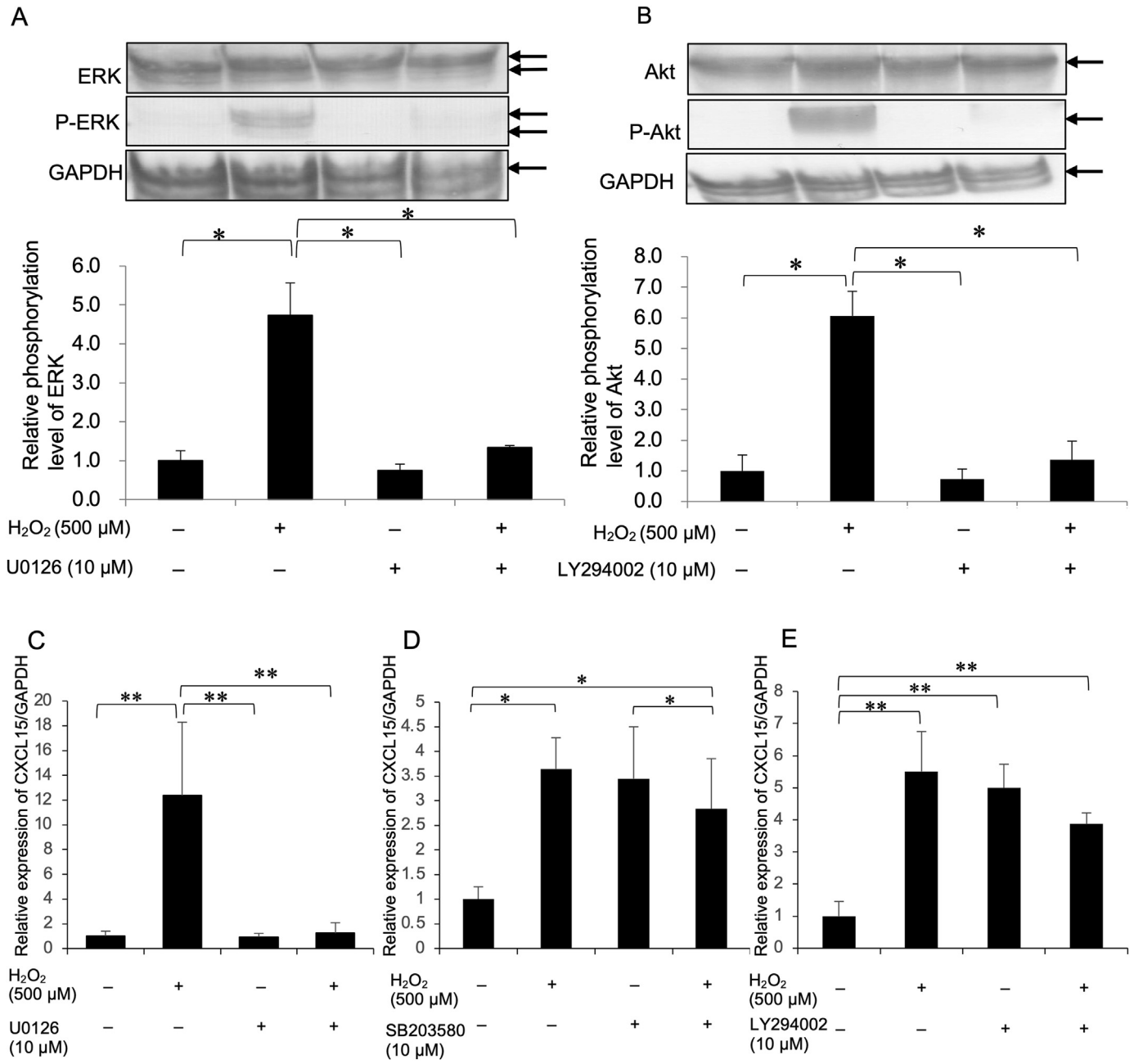


**Fig. 3.** MEK inhibitor and neither p38 MAPK inhibitor nor PI3K inhibitor suppressed $H_2O_2$-induced mRNA expression of CXCL15/Lungkine in FLS1 cells. Cells were treated with $H_2O_2$ (500 μM) for 24 h. (**A and C**) MEK inhibitor U0126 (10 μM), **(B and E)** PI3K inhibitor LY294002 (10 μM), or **(D)** p38 MAPK inhibitor SB203580 (10 μM) were added 30 min before $H_2O_2$ administration. **(A)** Levels of total (upper panel), and phosphorylated (middle panel) ERK1/2 levels were evaluated by western blot analysis. Relative levels of phosphorylated ERK1/2 against total levels of ERK1/2 were shown as the ratio of band intensity. **(B)** Levels of total (upper panel) and phosphorylated (middle panel) Akt were evaluated by western blot analysis. Relative levels of phosphorylated Akt against total levels of Akt were shown as the ratio of band intensity. **(A and B)** Data were presented as the mean ± SD (n = 3). *, $P < 0.01$. GAPDH levels (lower panel) were examined as a reference for the amount of protein loaded in each lane. **(C, D, and E)** Expression of CXCL15/Lungkine mRNA was evaluated by RT-qPCR analysis. Data were presented as the mean ± SD (n = 3). *, $P < 0.01$**; $P < 0.05$.

in chondrocytes, were converted to $H_2O_2$ in chondrocytes [24], suggesting that $H_2O_2$ is a major candidate as an oxidative stress inducer in OA.

We found that $H_2O_2$ (500 μM) increased the phosphorylation of ERK1/2, p38 MAPK, and Akt in FLS1 cells (Fig. 2A, B, and 2C). In addition, the MEK inhibitor U0126 (10 μM) completely reversed $H_2O_2$-mediated increase in mRNA expression of CXCL15/Lungkine in FLS1 cells (Fig. 3C); however, the same effect was not observed with p38 MAPK inhibitor SB203580 (10 μM) (Fig. 3D), and not with PI3K inhibitor LY294002 (10 μM) (Fig. 3E). These results strongly suggested that $H_2O_2$ induced a MEK/ERK1/2-mediated signal that promoted the mRNA expression of CXCL15/Lungkine, and also suggested that the $H_2O_2$-induced p38 MAPK-, or PI3K/Akt-mediated signals were not involved in promotion of CXCL15/Lungkine mRNA expression in FLS1 cells. In contrast, $H_2O_2$ (250 μM) has been reported to induce IL-8 expression through the activation of ERK1/2, p38 MAPK, and JNK in human periodontal ligament cells [11]. Importantly, the antioxidant NAC (5 mM), a precursor of GSH, partially but significantly reversed $H_2O_2$-mediated phosphorylation of ERK1/2 in FLS1 cells (Fig. 4B). Taken together, these results suggest that $H_2O_2$-induced oxidative stress upregulates CXCL15/Lungkine mRNA expression in FLSs in a MEK/

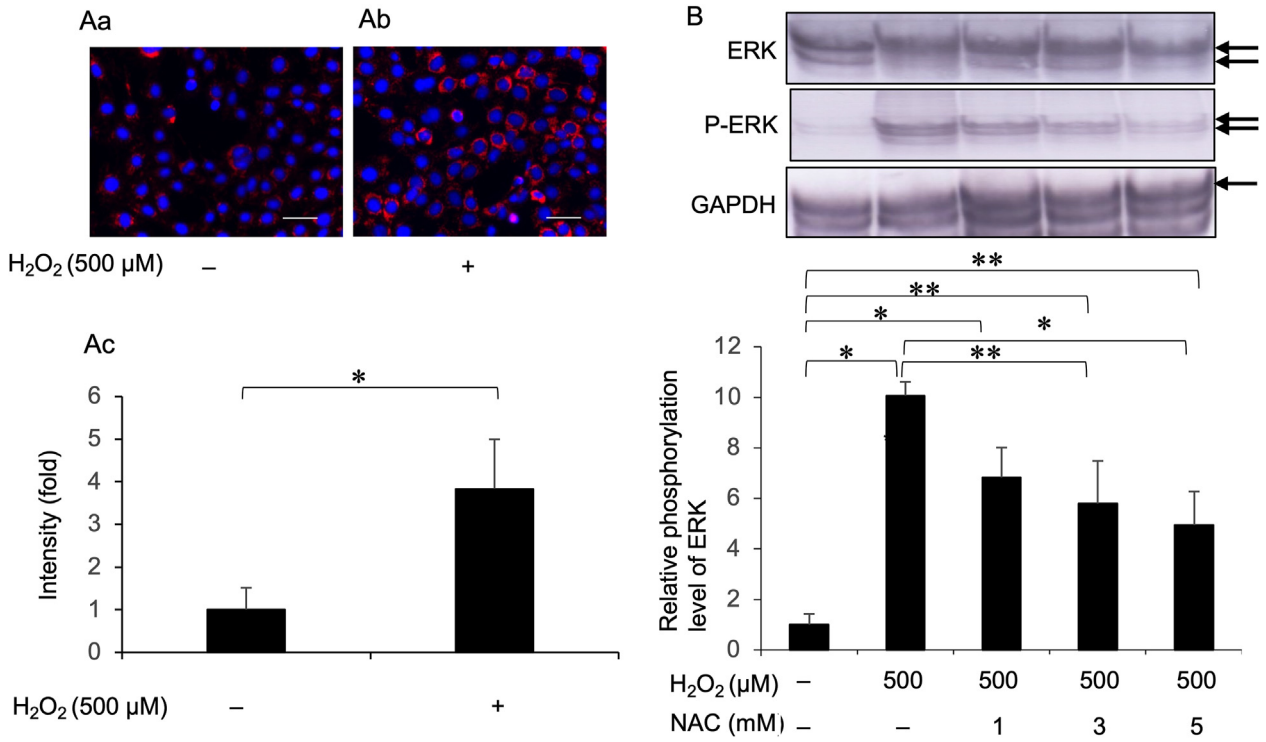


**Fig. 4.** Antioxidant NAC partially and significantly reverses the $H_2O_2$-mediated increase in phosphorylation of ERK1/2 in FLS1 cells. (A) Cells were cultured **(Aa)** without or **(Ab)** with $H_2O_2$ (500 μM) for 24 h, and then OH• production in the cells was fluorescently visualized as described in the Materials and methods section. The nuclei were counter-stained with Hoechst 33342 (blue). Scale bar, 50 μm. **(Ac)** Relative production of HO• in $H_2O_2$-treated cells against to that in non-treated cells was shown as the ratio of fluorescent intensity as described in the Materials and methods section. Data were presented as the mean ± SD (n = 6). *, $P < 0.01$. **(B)** Cells were incubated with or without $H_2O_2$ (500 μM) for 30 min and pretreated with the antioxidant *N*-acetyl-L-cysteine 30 min before $H_2O_2$ administration. Then, total (upper panel) and phosphorylated (middle panel) ERK1/2 levels were evaluated by western blot analysis. Relative levels of phosphorylated ERK1/2 against total levels of ERK1/2 were shown as the ratio of band intensity. Data were presented as the mean ± SD (n = 3). *, $P < 0.01$; **, $P < 0.05$. GAPDH levels (lower panel) were examined as a reference for the amount of protein loaded in each lane.

ERK1/2-dependent manner. Unexpectedly, NAC (5 mM) did not reverse $H_2O_2$-induced upregulation of CXCL15/Lungkine mRNA expression in FLS1 cells (data not shown), suggesting that the partial reduction in $H_2O_2$-mediated phosphorylation of ERK1/2 might not be sufficient to inhibit $H_2O_2$-mediated upregulation of CXCL15/Lungkine mRNA expression. However, NAC administration reportedly promotes IL-8 expression through activation of the transcription factor erythroid 2-related factor 2 (Nrf2) in a cell type-specific manner: Wang et al. demonstrated that NAC injection ameliorated carrageen-induced prostate inflammation and pain by promoting Nrf2 expression in rats [25]. In addition, Jannatifar et al. reported that oral NAC supplementation significantly promoted Nrf2 expression in the sperm of patients with asthenoteratozoospermia [26]. Intriguingly, Zhang et al. demonstrated that Nrf2 overexpression in human kidney mesangial cells promoted IL-8 mRNA expression by increasing the half-life of IL-8 mRNA [27]. In light of these previous findings, it seems plausible that NAC administration might promote CXCL15/Lungkine mRNA expression through the upregulation of Nrf2 expression in FLSs. In contrast, NAC has been reported to reverse $H_2O_2$-induced suppression of osteoblastic differentiation of mouse osteoblastic cells via downregulation of Nrf2 expression [28]. Therefore, NAC can upregulate or downregulate Nrf2 expression, which possibly results in upregulation or downregulation of CXCL15/Lungkine mRNA expression, respectively, in a cell- and tissue-specific manner.

Here, we showed that there was possibility that ERK1/2-mediated signal related molecules could be molecular targets for the establishment of novel therapies that suppress the development of inflammatory lesions of TMJ-OA: inhibitors against to ERK1/2-mediated signal transduction molecules might retain an ability to suppress the oxidative stress-promoted expression of CXCL15/Lungkine mRNA, resulting in inhibition of infiltration of inflammatory cells to lesions of TMJ-OA. In addition, we have to elucidate whether the antioxidants other than NAC retain an ability to abrogate both the $H_2O_2$-promoted phosphorylation of ERK1/2 and the $H_2O_2$-induced expression of CXCL15/Lungkine mRNA near future.

## 5. Conclusion

In summary, we found that $H_2O_2$-induced oxidative stress promotes the expression of CXCL15/Lungkine mRNA in a MEK/ERK-dependent manner in FLSs derived from mouse TMJ, suggesting that FLSs recruit neutrophils to TMJ-OA lesions through production of CXCL15/Lungkine thereby exacerbating the local inflammatory response. Our findings provide insights into the molecular mechanisms underlying the development of inflammatory lesions in TMJ-OA.

## CRediT authorship contribution statement

**Kanna Asanuma:** Conceptualization, data analysis, interpretation, and writing, review, and editing. **Seiji Yokota:** Conceptualization, methodology, data analysis, and interpretation. **Naoyuki Chosa:** Data analysis and interpretation. **Masaharu Kamo:** Data analysis and interpretation. **Miho Ibi:** Methodology, data analysis, and interpretation. **Hisayo Mayama:** Data analysis and interpretation. **Tarou Irié:** Methodology, data analysis, and interpretation. **Kazuro Satoh:** Conceptualization, data analysis, and interpretation.

**Akira Ishisaki:** Conceptualization, data analysis, interpretation, and writing, review, and editing.

## Ethical approval

All authors declare that ethical approval is not required for this original article.

## Conflicts of interest

There are no conflicts of interest to declare.

## Acknowledgements

We thank Prof. Eiichi Taira for data interpretation of hydroxyl radical detection using fluorescence microscopy. This work was supported by the Japan Society for the Promotion of Science KAKENHI grants (no. 19K19277 [S.Y.], no. 20K10234 [H.M.], and no. 20K09883 [A. I.]).

## References

[1] Kalladka M, Quek S, Heir G, Eliav E, Mupparapu M, Viswanath A. Temporomandibular joint osteoarthritis: diagnosis and long-term conservative management: a topic review. J Indian Prosthodont Soc 2014;14:6–15. https://link.springer.com/article/10.1007/s13191-013-0321-3.

[2] Xia B, Di C, Zhang J, Hu S, Jin H, Tong P. Osteoarthritis pathogenesis: a review of molecular mechanisms. Calcif Tissue Int 2014;95:495–505. https://link.springer.com/article/10.1007/s00223-014-9917-9.

[3] Tipton DA, Christian J, Blumer A. Effects of cranberry components on IL-1β-stimulated production of IL-6, IL-8 and VEGF by human TMJ synovial fibroblasts. Arch Oral Biol 2016;68:88–96. https://doi.org/10.1016/j.archoralbio.2016.04.005.

[4] Zhou PH, Qiu B, Deng RH, Li HJ, Xu XF, Shang XF. Chondroprotective effects of hyaluronic acid-chitosan nanoparticles containing plasmid DNA encoding cytokine response modifier A in a rat knee osteoarthritis model. Cell Physiol Biochem 2016;47:1207–16. https://doi.org/10.1159/000490217.

[5] Li D, Wang W, Xie G. Reactive oxygen species: the 2-edged sword of osteoarthritis. Am J Med Sci 2021;344:486–90. https://doi.org/10.1097/MAJ.0b013e3182579dc6.

[6] Henrotin Y, Kurs B, Aigner T. Oxygen and reactive oxygen species in cartilage degradation: friends or foes? Osteoarthritis Cartilage 2005;13:643–54. https://doi.org/10.1016/j.joca.2005.04.002.

[7] Jiang C, Luo P, Li X, Liu P, Li Y, Xu J. Nrf2/ARE is a key pathway for curcumin-mediated protection of TMJ chondrocytes from oxidative atress and inflammation. Cell Stress Chaperones 2020;25:395–406. https://doi.org/10.1007/s12192-020-01079-z.

[8] Setti T, Arab MGL, Santos GS, Alkass N, Andrade MAP, Lana JFSD. The protective role of glutathione in osteoarthritis. J Clin Orthop Trauma 2021;15:145–51. https://doi.org/10.1016/j.jcot.2020.09.006.

[9] Molnar V, Matišić I, Bjerica R, Jeleč Ž, Hudetz D, Rod E, et al. Cytokines and chemokines involved in osteoarthritis pathogenesis. Int J Mol Sci 2021;22:9208. https://doi.org/10.3390/ijms22179208.

[10] Roebuck KA. Oxidant stress regulation of IL-8 and ICAM-1 gene expression: differential activation and binding of the transcription factors AP-1 and NF-kappaB (Review). Int J Mol Med 1999;4:223–30. https://doi.org/10.3892/ijmm.4.3.223.

[11] Lee YS, Bak EJ, Kim M, Park W, Seo JT, Yoo YJ. Induction of IL-8 in periodontal ligament cells by H(2)O(2). J Microbiol 2008;46:579–84. https://doi.org/10.1007/s12275-008-0182-3.

[12] Luigi DL, Sgró P, Duranti G, Sabatini S, Caporossi D, Galdo FD, et al. Sildenafil reduces expression and release of IL-6 and IL-8 induced by reactive oxygen species in systemic sclerosis fibroblasts. Int J Mol Sci 2020;21:3161. https://doi.org/10.3390/ijms21093161.

[13] Jeong JY, Lee YJ, Han JH, Park SY, Hwang KW, Sohn UD. The inhibitory effect of PIK-75 on inflammatory mediator response induced by hydrogen peroxide in feline esophageal epithelial cells. Mediat Inflamm 2014;2014:178049. https://doi.org/10.1155/2014/178049.

[14] Chen X, Chen R, Jin R, Huang Z. The role of CXCL chemokine family in the development and progression of gastric cancer. Int J Clin Exp Pathol 2020;13:484–92. https://www.ncbi.nlm.nih.gov/pmc/articles/PMC7137023/pdf/ijcep0013-0484.pdf.

[15] Rossi DL, Hurst SD, Xu Y, Wang W, Menon S, Coffman RL, et al. Lungkine, a novel CXC chemokine, specifically expressed by lung bronchoepithelial cells. J Immunol 1999;162:5490–7. http://www.jimmunol.org/content/162/9/5490.

[16] Chen SC, Mahrad B, Deng JC, Vassileva G, Manfra DJ, Cook DN, et al. Impaired pulmonary host defense in mice lacking expression of the CXC chemokine Lungkine. J Immunol 2001;166:3362–8. http://www.jimmunol.org/content/166/5/3362.

[17] Schmitz JM, McCracken VJ, Dimmitt RA, Lorenz RG. Expression of CXCL15 (Lungkine) in murine gastrointestinal, urogenital, and endocrine organs. J Histochem Cytochem 2007;55:515–24. https://doi.org/10.1369/jhc.6A7121.2007.

[18] Yokota S, Chosa N, Kyakumoto S, Kimura H, Ibi M, Kamo M, et al. ROCK/actin/MRTF signaling promotes the fibrogenic phenotype of fibroblast-like synoviocytes derived from the temporomandibular joint. Int J Mol Med 2017;39:799–808. https://doi.org/10.3892/ijmm.2017.2896.

[19] Roskoski RJ. ERK1/2 MAP kinases: structure, function, and regulation. Pharmacol Res 2012;66:105–43. https://doi.org/10.1016/j.phrs.2012.04.005.

[20] Doza YN, Cuenda A, Thomas GM, Cohen P, Nebreda AR. Activation of the MAP kinase homologue RK requires the phosphorylation of Thr-180 and Tyr-182 and both residues are phosphorylated in chemically stressed KB cells. FEBS Lett 1995;364:223–8. https://doi.org/10.1016/0014-5793(95)00346-B.

[21] Gkouveris I, Nikitakis NG. Role of JNK signaling in oral cancer: a mini review. Tumor Biol 2017;39:1010428317711659. https://doi.org/10.1177/1010428317711659.

[22] Risso G, Blaustein M, Pozzi B, Mammi P, Srebrow A. Akt/PKB: one kinase, many modifications. Biochem J 2015;468:203–14. https://doi.org/10.1042/BJ20150041.

[23] Ueno T, Yamada M, Sugita Y, Ogawa T. *N*-acetyl cysteine protects TMJ chondrocytes from oxidative stress. J Dent Res 2011;90:353–9. https://doi.org/10.1177/0022034510388035.

[24] Hiran TS, Moulton PJ, Hancock JT. Detection of superoxide and NADPH oxidase in porcine articular chondrocytes. Free Radic Biol Med 1997;23:736–43. https://doi.org/10.1016/S0891-5849(97)00054-3.

[25] Wang LL, Huang YH, Yan CY, Wei XD, Hou JQ, Pu JX, et al. *N*-acetylcysteine ameliorates prostatitis via miR-141 regulating Keap1/Nrf2 signaling. Inflammation 2016;39:938–47. https://doi.org/10.1007/s10753-016-0327-1.

[26] Jannatifar R, Parivar K, Roodbari NH, Nasr-Esfahani MH. The effect of *N*-acetylcysteine on Nrf2 antioxidant gene expression in asthenoteratozoospermia men: a clinical trial study. Int J Fertil Steril 2020;14:171–5. https://www.ijfs.ir/article_46174.html.

[27] Zhang X, Chen X, Song H, Chen HZ, Rovin RH. Activation of the Nff2/antioxidant response pathway increases IL-8 expression. Eur J Immunol 2005;35:3258–67. https://doi.org/10.1002/eji.200526116.

[28] Lee D, Kook SH, Ji H, Lee SA, Choi KC, Lee KY, et al. *N*-acetyl cysteine inhibits $H_2O_2$-mediated reduction in the mineralization of MC3T3-E1 cells by down-regulating Nrf/HO-1 pathway. BMB Rep 2015;48:636–41. https://doi.org/10.5483/BMBRep.2015.48.11.112.